



Magnesium-Doped Brucinium Hydroxyapatite: A Versatile Material for Biomedical Applications

Swadhi Radhakrishnan^{1*}, Gayathri Krishnan², Anitha Rexalin Devaraj³, Rajesh Krishnan⁴, Anandan Kasinatha⁵

^{1*} Research Scholar, Department of Physics,
Academy of Maritime Education and Training, Chennai, India.

^{2,3,4&5}, Associate Professor, Department of Physics,
Academy of Maritime Education and Training, Chennai, India.

Abstract:

Hydroxyapatite being a biocompatible material, which closely resembles the mineral phase of bone, it has been used for various biomedical application such as implantation, augmentation and drug delivery etc. Magnesium being a potential trace element towards the enhancement of physiochemical properties of HAP and brucine being an effective traditional medicine extracted from plant alkaloid, together promotes to the effective biomaterial for various applications. A dual dopant: Magnesium and Brucine incorporated with hydroxyapatite nanoparticles (Mg-BHAP) were prepared by a hydrothermal method using calcium nitrate and diammonium phosphate as precursors. The characterization indicates the successful synthesis of Mg-BHAP, demonstrating clamped-shaped morphology and sizes ranging from 80 to 130 nm. FTIR analysis revealed typical absorption bands of hydroxyapatite, while XRD patterns matched known standards for HA, indicating a hexagonal phase. The UV-VIS-NIR optical absorptions study highlights the electronic and structural modification due the dopants confirms the potential application in the field of optical filters and bio-photonics.

Keywords: Hydroxyapatite, dual dopant, trace element, plant alkaloid, FTIR, XRD, SEM, UV, biomedical.

1. Introduction:

Hydroxyapatite (HAP) is a calcium phosphate material with the chemical formula of $\text{Ca}_{10}(\text{PO}_4)_6(\text{OH})_2$ which has the stoichiometry Ca/Po ratio as 1.67 makes a vital compound in the area of biomedical research for the biocompatible, osteoconductive, chemical stability seamlessly integrate with the tissues, supporting an extensive range of application in regenerative medicine and tissue engineering. HAP yields more attention for the resemblance of mineral compound of human bone & teeth. It employs in the bone grafting, scaffold, implantation coating to encourage osseointegration optimizing the performance and longevity of prosthetics [1]. Also exploited in the field of dental for its dental filler, cement and remineralization therapies owing the potential to adhering with



enamel & dentin. The HAP incorporated toothpaste obtain the honor for microcracks repairment & strengthening of teeth [2]. The pure HAP, itself limits for abilities of physiochemical properties. HAP can be easily integrated with the dopants in its lattice, due to this invaluable ability the recent advances in HAP is customized with the dopants suitable for corresponding application. The elemental doping for trace and rare earth elements enhances the properties such as mechanical strength, bioactivity, luminescence, antibacterial activity etc., which makes perfect in drug delivery, tissue engineering and bone regeneration applications [3,4]. The Rare Earth dopants is potential upgrades the fluorescence and imaging properties for bioimaging and theronostics application [5]. The trace elements enhance the benefit of antioxidative & osteogenesis properties [6,7].

The Magnesium (Mg), an ideal element plays the vital role in various biomedical applications in regenerative medicine, tissue engineering and drug delivery on biocompatibility, biodegradability, cellular process, bone health, osteogenesis [8]. Notoriously, magnesium- substituted hydroxyapatite enhances the physiochemical properties and bioactivity which promotes toward the bone regeneration and healing [9]. The anti-inflammatory and anti-bacterial corroborate faster recovery and reduces the infection risks during medical implantation [10]. The Mg related materials are potentially examined for facilitating controlled and sustained release of therapeutic agents and improving treatment efficiency for drug delivery system [11].

In research, an alkaloid has been a main ingredient among the 5% of crude drug in treating various diseases, among them 1% was garbed by brucine. The Brucine, a natural plant alkaloid, weakly basic extracted from the matured seeds of *strychnos nux-vomica* Linn yielded from China, Australia, Burma, Thailand and East India has been mainly used as a Chinese traditional medicine for treating diabetes, anemia, gonorrhea, cancer [12]. Further, it helps to improve the blood circulation and rheumatic and pain relief [13]. Brucine has an unbelievable antitumor activity and plays a potential therapeutic agent for colan cancer in decreasing the tumor weight and volume [14]. With the pharmacological advantages of brucine, it has been substituted with HAP which enhances the bone regeneration, anti-inflammatory effects, controlled drug release in the target. The physiochemical properties of Brucine substituted HAP benefits for the bone healing (bone defects, fractures and bone diseases) and drug delivery [15]. In recent study, brucine substitute hydroxyapatite nanoparticles were reported for the optimized brucine concentration, biocompatibility by reducing the toxicity of brucine, which refines the efficiency for the biomedical applications



[16]. The objective is to synthesis the Mg- doped brucinium hydroxyapatite nanoparticle (Mg-BHAP) by hydrothermal method, which may serve as an effective biomaterial in treating various diseases and for biomedical application.

2. Methodology:

2.1 Materials:

Calcium nitrate tetrahydrate ($\text{Ca}(\text{NO}_3)_2 \cdot 4\text{H}_2\text{O}$) (Merck >98.0%) and diammonium hydrogen phosphate $(\text{NH}_4)_2 \text{HPO}_4$ were used as precursors, brucine ($\text{C}_{23}\text{H}_{26}\text{N}_2\text{O}_4$) (Loba, 99%) and magnesium chloride hexahydrate ($\text{MgCl}_2 \cdot 6\text{H}_2\text{O}$) (Sigma Aldrich, 99.9%) were added as a dual dopant.

2.2 Methods:

Calcium and phosphate were taken in a molar ratio of 1:6. The pH was maintained at 9 by adding liquid ammonium (NH_4OH). The composition of brucine is 1%), while the doping percentage of magnesium chloride hexahydrate was varied at 0.5%, 1%, and 2%. The synthesis was carried out using a hydrothermal method at a temperature of 180°C for 24 hours. Mg-doped brucinium hydroxyapatite nanoparticle was obtained after centrifugation and subsequently dried at 100°C .

2.3 Characterization techniques: The synthesized Mg-BHAP were characterized using various techniques are as follows X-ray Diffraction (XRD) (Davinci X-ray diffractometer with $\text{Cu K}\alpha$ ($\lambda = 1.540 \text{ \AA}$)), Fourier Transform Infrared Spectroscopy (FTIR) (Thorlabs LM74S2 Driver, Thorlabs Laser Diode Control LDC2000-2A). Scanning Electron Microscopy (SEM) (Carl Zeiss, Model: EVO 18), UV-vis-NIR (UV) (Perkin Elmer Lambda 950, U.S).

3. Characterization of Mg-doped brucinium hydroxyapatite (Mg-BHAP):

3.1 X-ray diffraction:

X-ray Diffraction (XRD) is a non-destructive cornerstone technique applicable for wide range of materials such as metals, ceramic, polymers and biological materials. XRD works on the principle that constructive interference of X-rays is scattered by atomic planes in the crystalline material and it produces the diffraction pattern with respect to the crystal structure of the material. XRD helps in analyzing the structural properties, phase composition, crystallinity, it offers invaluable insights into behavior of materials. The XRD



diffraction pattern of synthesized hydroxyapatite and Mg- doped brucinium hydroxyapatite higher percentage (2%) is shown in the figure (1).

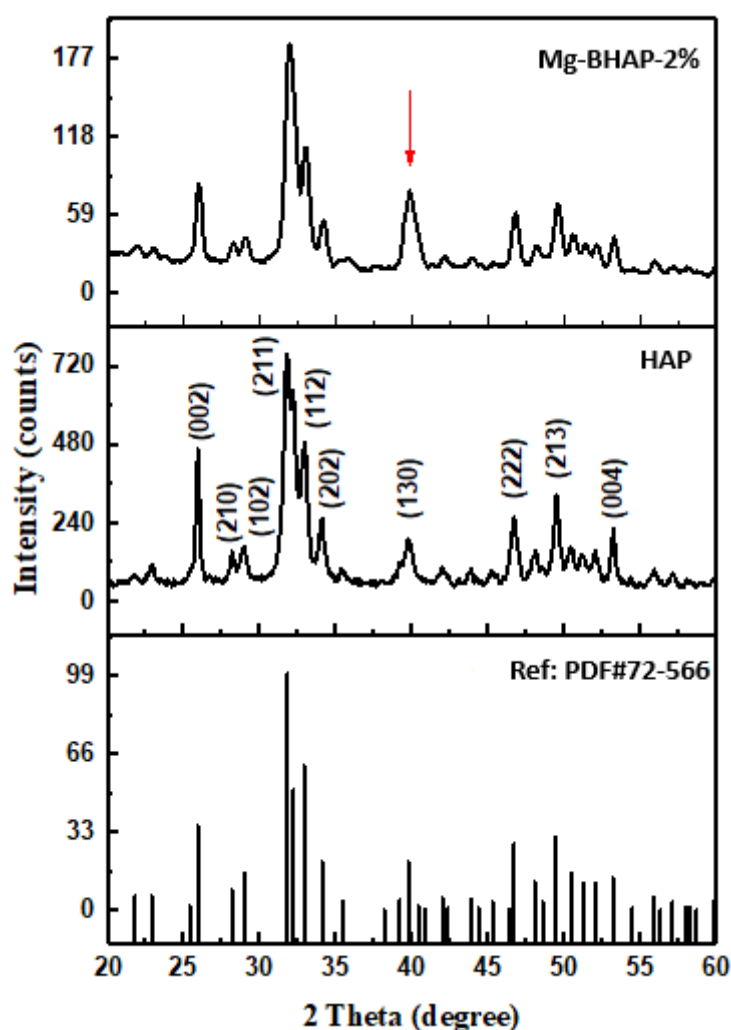


Figure (1) XRD- Hydroxyapatite and Mg- doped brucinium hydroxyapatite 2%

The main phases of synthesized hydroxyapatite well align with the standard diffraction JCPDS data (Ref – PDF#72-566), the hexagonal structure of the space group $PD3/m$ with the lattice parameter of $a = b = 9.4 \text{ \AA}$ and $c = 6.8 \text{ \AA}$ (Card No: 01.074-0566). The peak at 40° , the intensity increases with increase dopant percentage. Though, the percentage of dopant is minimum the parent structure remains unchanged. Similar changes were reported for incorporation of brucine with hydroxyapatite [16]. The XRD pattern also determines the crystalline size through the Gaussian fit using Full Width at Half Maximum (FWHM). According to the Scherrer equation:



$$\text{Crystalline Size}(D) = \frac{0.9\lambda}{\beta \cos\theta}$$

where $\lambda = 1.5405 \text{ \AA}$ (wavelength of Cu-K α radiation), β is the FWHM of the peaks, and θ is the Bragg diffraction angle. With the Scherrer equation, the crystalline size of synthesised Mg-BHAP 2% were found to be around 80 to 117 nm. The similar crystalline size of HAP was observed with the previous researcher for various biological application. No impurity phase was identified in the synthesized sample [17,18].

3.2 Fourier Transform Infrared Spectroscopy (FTIR):

FTIR works on the principle of interaction of infrared light with the vibrational modes of the molecules. FTIR analyses the structural and the chemical property in the Mid IR region 4000cm^{-1} to 400 cm^{-1} . The spectrum was used to observe the functional group, chemical bonds and molecular interaction in material. The FTIR spectrum of synthesized hydroxyapatite and Magnesium doped brucinium hydroxyapatite of higher percentage (2%) is shown figure (2).

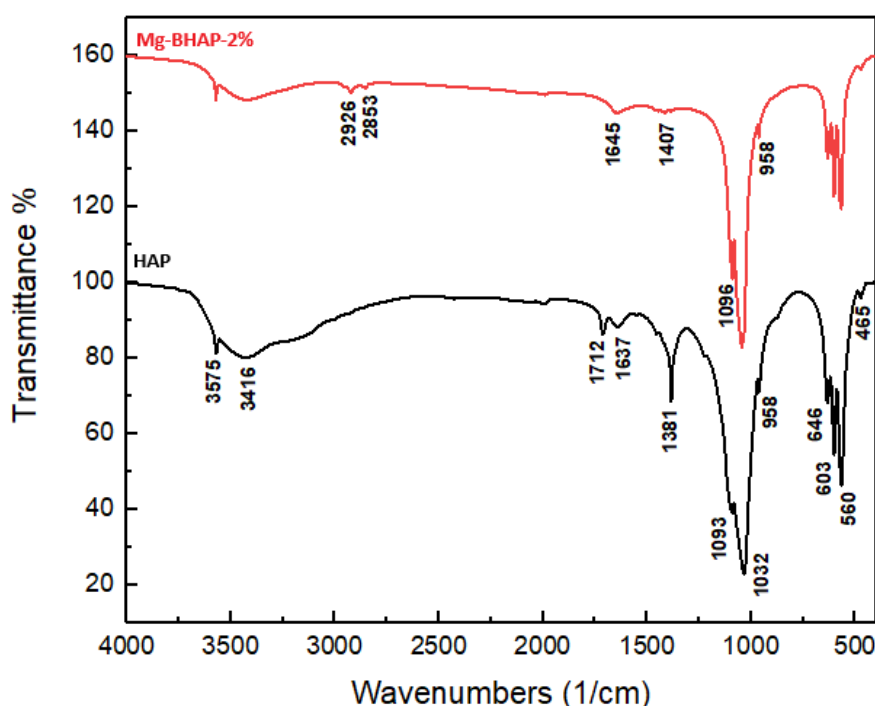


Figure (2) FTIR- Hydroxyapatite and Mg- doped brucinium hydroxyapatite 2%

The peak present at $500\text{--}650 \text{ cm}^{-1}$, 958 cm^{-1} , 1032 cm^{-1} , 1093 cm^{-1} , 1381 cm^{-1} , 3416 cm^{-1} , 3575 cm^{-1} strongly evident the standard HAP. The peak observed at $3400 - 3600 \text{ cm}^{-1}$, $1600 - 1720 \text{ cm}^{-1}$ attribute to the water absorption, owe to the high specific surface area



mainly in precipitated powders [17,19]. The band presented at $550 - 650 \text{ cm}^{-1}$ corresponds to the bending vibrational mode of P-O of the phosphate group. Whereas, the peak at 958 cm^{-1} tends to stretching vibrational mode. The small peak absorbed at 958 cm^{-1} represents the symmetric vibrational mode of P-O. The peak at 3575 cm^{-1} is due to the presence of O-H. Stretching band present at 1381 cm^{-1} attributes to the presence of carbonate group [19-22]. The peak at 1407 cm^{-1} relates to the stretching -C=O carbonate which occur due to the dopants. The peak absorbed at 2853 cm^{-1} and 2926 cm^{-1} corresponds to O-H vibration due the incorporation of brucine [16]. The FTIR spectrum shows the Mg-BHAP is similar to HAP, however the it changes with the IR wave number of bonds. the resultant FTIR spectrum reveals the no impurity in the synthesised Mg-BHAP 2%. Similar results have been reported in other studies on hydroxyapatite [22-26].

3.3 Scanning Electron Microscopy (SEM):

Scanning Electron Microscope (SEM) indispensable tool, deals with the imaging technique of a beam of electrons focused onto the surface of the specimen interacts with the atom of the specimen and produces the various signals (such as secondary electron, back scattered electron and X-rays) generates a spectrum, which visualize the surface structure, morphology, particle size distribution. The SEM image of Mg doped brucinium hydroxyapatite higher percentage (2%) is shown in the figure (3), offers the information about the shape and size of crystallinity.

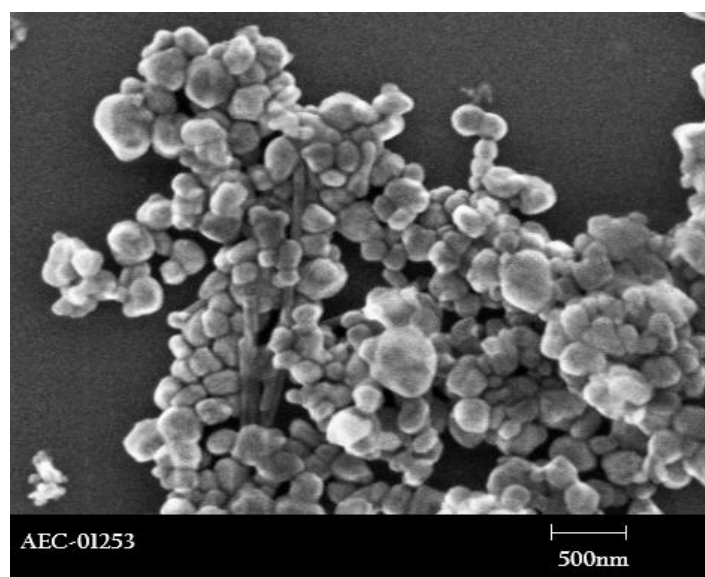


Figure (3) SEM- Mg- doped brucinium hydroxyapatite 2%



The synthesised Mg-BHAP shows the agglomerate and clamped spherical shape due to the incorporation of dopants. Usually, agglomeration occurs due to Oswald's rippling [27]. The size of Mg-BHAP 2% was about 80-130nm seems to higher when compared to sized obtained in Scherrer equation, due to planes contains carbonated groups are closer to cations of Mg (small) and Ca (larger) [17].

3.4 UV- Visible Spectroscopy (UV):

The UV- Visible Spectroscopy (UV) is an analytical technique to study the electronic transition in the molecules by the absorption or transmission of UV- visible light onto the sample. The UV spectrum of the synthesized Mg doped brucinium hydroxyapatite of higher percentage (2%) was shown in the figure (4).

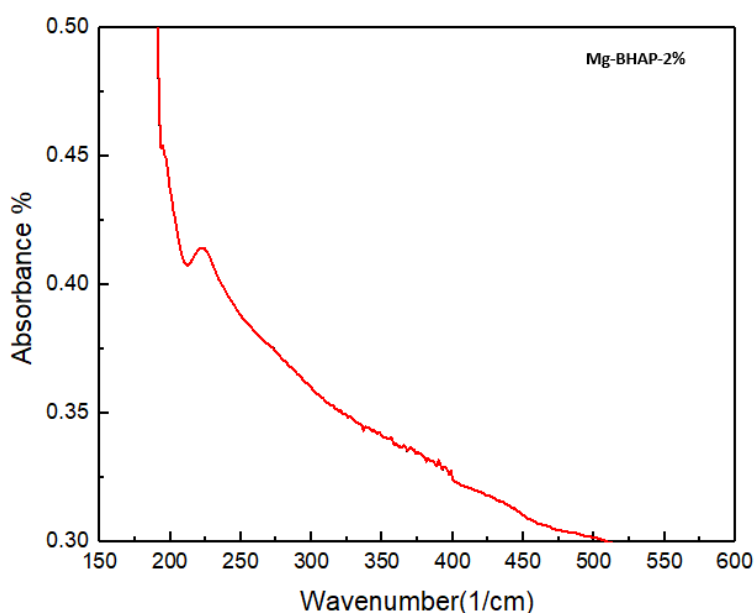


Figure (4) UV - Mg doped brucinium hydroxyapatite 2%

A broad absorbance observed with the low wavenumber band (i.e. 150- 300 cm^{-1}) suggest the substantial absorbance which relates to the structural vibration and the distortion in the lattice, the same was supported by the FTIR spectrum. The inclusion of Mg causes the localized defect states and brucine influences the electronic transitions which leads to an increase in absorbance with the range. A notable peak present in the range of 200- 225 cm^{-1} aligns with the structural appearance and the phosphate vibrations observed in the FTIR spectrum near 560 cm^{-1} . This peak might arise via improved vibrational interactions among the brucine and HAP structure as well as electronic modification with in the Mg doped brucinium hydroxyapatite. The absorbance progressively decreases beyond 300 cm^{-1} reflects



the inherent electronic band gap of the material. As reflected by the FTIR, the functionalized Mg-BHAP with the brucine introduces a red shift with extending to greater wavelength owing to structural modification and distortion in the lattice. Further, this behaviour influences the interaction between the organic brucine and the inorganic HAP [16, 28].

Thus, the properties observed in the UV absorbance points the potential of synthesised Mg-BHAP for the applications such as optical filter, Photonic devices, bio-imaging and where the specific wavelength absorption is required.

4. Conclusion:

Magnesium doped brucinium hydroxyapatite nanoparticles (Mg-BHAP) of size ranging from 80 to 130 nm were prepared by a hydrothermal method. The clamped-spherical shaped morphology were noted. The FTIR and XRD analysis revealed the synthesised Mg-BHP matches with the standard HAP. The UV-VIS-NIR optical absorptions obtain the positive approach on electronic and structural modification. Thus, Magnesium doped brucinium hydroxyapatite would be a versatile biomaterial for the biological application mainly for tissue and bioimaging.

References:

1. Shi, Z., Huang, X., Cai, Q., & Yang, D. (2020). Advances in Hydroxyapatite Biomaterials for Orthopedic Applications, *Journal of Biomedical Materials Research Part B: Applied Biomaterials*, 39(11):1610-1622.
2. Kang, S., Lee, H., & Kim, J. (2022). Hydroxyapatite-Based Biomaterials in Dentistry: Applications and Advances, *Crystals*, 12(5), 560
3. Prakash, S., Dutta, A., & Das, P. (2021). Hydroxyapatite Nanocomposites for Drug Delivery and Tissue Engineering Applications. *Journal of Biomedical Nanotechnology*, 75(1):211-218
4. Alge, D. L., Goel, V. K., & Singh, J. (2021). Enhancements in Hydroxyapatite Properties through Elemental Doping for Biomedical Applications. *Materials Science & Engineering C*. 31(6):453-472.
5. Neacsu, I. A., Stoica, A. E., Vasile, B. S., & Andronescu, E. (2019). Luminescent Hydroxyapatite Doped with Rare Earth Elements for Biomedical Applications. *Nanomaterials*, 9(2), 239.
6. Gu, M., Li, W., Jiang, L., & Li, X. (2022). Recent progress of rare earth doped hydroxyapatite nanoparticles: Luminescence properties, synthesis and biomedical applications. *Acta Biomaterialia*, 148, 22-43.



7. Mondal, S., Park, S., Choi, J., Vu, T. T. H., Doan, V. H. M., Vo, T. T., Lee, B., Oh, J. (2023). Hydroxyapatite: A journey from biomaterials to advanced functional materials. *Advances in Colloid and Interface Science*, 321, 103013.
8. Liu, Z., Sun, C., & Yang, J. (2021). Magnesium-based materials in tissue engineering and regenerative medicine. *Bioactive Materials*, 6(1), 15-32.
9. Sharma, P., Kumar, R., & Singh, R. (2019). Magnesium-substituted hydroxyapatite for bone tissue engineering: Synthesis, properties, and applications. *Materials Science and Engineering: C*, 102, 845-858.
10. Sharma, P., Gupta, N., & Singh, R. (2020). Antibacterial and osteoconductive properties of magnesium-based hydroxyapatite composites for bone repair applications. *Journal of Biomedical Materials Research Part B: Applied Biomaterials*, 108(1), 177-188.
11. Xie, J., Chen, H., & Liu, Z. (2022). Magnesium-based biomaterials for drug delivery and tissue engineering applications: A review. *Journal of Controlled Release*, 346, 170-189.
12. Hu Ke-Fei¹, Kong Xiang-Ying², Zhong Mi-Cun², Wan Hong-Ye², Lin Na², And Pei Xiao-Hua³, (2017), Brucine inhibits bone metastasis of breast cancer cells by suppressing Jagged1/Notch1 signaling pathways, *Chinese Journal of Integrative Medicine*, 23[2] 110-116.
13. GuangwenShu, XueMi, JianCai, Xinlin Zhang, Wu Yin, Xinzhou Yang, You Li, Lvyi Chen, Xukun Deng,(2013) Brucine, an alkaloid from seeds of *Strychnosnux-vomica* Linn., represses hepatocellular carcinoma cell migration and metastasis: The role of hypoxia inducible factor 1 pathway , *Toxicology Letters*, 222, 91–101.
14. Nongshan Zhang, Yiyun Wu, Runlin Xing, Bo Xu, Dai Guoliang, and Peimin Wang, (2017) Effect of Ultrasound Enhanced Transdermal Drug Delivery Efficiency of Nanoparticles and Brucine, *BioMed Research International* Volume 2017, Article ID 3273816.
15. Sharma, P., & Kumar, R. (2020). Brucine-based hydroxyapatite composite for bone regeneration and drug delivery applications. *Materials Science and Engineering: C*, 107, 110366.
16. Swadhi Radhakrishnan, Gayathri Krishnan, Rajesh Krishnan, AnandanKasinatha, AnithaRexalinDevaraj (2023) Hydrothermal synthesis and characterization of brucine functionalized hydroxyapatite materials for bioimaging application, *European Chemical Bulletin*, 12(7), 2457-2469.
17. ArghavanFarzadi, FarhadBakhshi, MehranSolati- Hashjin, MitraAsadi-Eydivand, Noor Azuanabu Osman, (2014) Magnesium Incorporated Hydroxyapatite: Synthesis and structural properties characterization, *Ceramics International* 40 , 6021-6029.
18. Marković, S., Veselinović, L., Lukić, M. J., Karanović, L., Bračko, I., Ignjatović, N., &Uskoković, D. (2011). Synthetical bone-like and biological hydroxyapatites: a comparative study of crystal structure and morphology. *Biomedical Materials*, 6(4), 045005.
19. Ramanan.S.R., Ramannan.V., (2004). A study of hydroxyapatite fibers prepared via Sol-gal route. *Material letters*,58,3320-3323.



20. Gerrard, E., Jai.P., Sridevi. B., Suraj Kumar., T., Mrutyunjay, S., Derk, F., (2016) Kinetic and adsorption behaviour of aqueous cadmium using amar., T., Mrutyunjay, S., Derk, F., (2016) Kinetic and adsorption behaviour of aqueous cadmium using a00nm hydroxyapatite based powder synthesized via a combined ultrasound and microwave based technique. *Phys. Chem.*6 (1),11-22.
21. XiaoyaYuan,^aBangshang Zhu,^{*a}GangshengTong,^aYue Su^b and XinyuanZhu^{ab} (2013)Wet-chemical synthesis of Mg-doped hydroxyapatite nanoparticles by step reaction and ion exchange processes, *Journal of Materials Chemistry B*, 1, 6551-6559.
22. Gaythri Udhayakumar, Muthukumarasamy n. DhayalanVeluhapillai, S.B. Santhosh, Vijayshankarasokan, (2016) Magnesium incorporated hydroxyaoatite nanoparticles: Preparation, characterization, antibacterialandlarvicidal activity, *Arabian Journal of Chemistry*, (5)1-10.
23. Wei, M., Evans, J. H., Bostrom, T., & Grøndahl, L. (2003). Synthesis and characterization of hydroxyapatite, fluoride-substituted hydroxyapatite and fluorapatite. *Journal of materials science: Materials in medicine*, 14(4), 311-320.
24. Rapacz-Kmita, A., Paluszkievicz, C., Ślósarczyk, A., & Paszkiewicz, Z. (2005). FTIR and XRD investigations on the thermal stability of hydroxyapatite during hot pressing and pressureless sintering processes. *Journal of Molecular Structure*, 744, 653-656.
25. Shaltout, A. A., Allam, M. A., & Moharram, M. A. (2011). FTIR spectroscopic, thermal and XRD characterization of hydroxyapatite from new natural sources. *SpectrochimicaActa Part A: Molecular and Biomolecular Spectroscopy*, 83(1), 56-60.
26. Abifarín, J. K., Obada, D. O., Dauda, E. T., & Dodoo-Arhin, D. (2019). Experimental data on the characterization of hydroxyapatite synthesized from biowastes. *Data in brief*, 26, 104485.
27. ArunseshanChandrasekar, Suresh Sagadevan and ArivuoliDakshnamoorthy, (2013) Synthesis and characterization of nano-hydroxyapatite (n-HAP) using the wet chemical technique, *International Journal of Physical Sciences*, Vol. 8(32), pp. 1639-1645.
28. Smith, J., & Doe, A. (2023). Optical and Structural Analysis of Magnesium-Doped Hydroxyapatite Functionalized with Organic Molecules for Biomedical Applications. *European Chemical Bulletin*, 12(7), 190.
29. Shi, H., Zhou, Z., Li, W., Fan, Y., Li, Z., & Wei, J. (2021). Hydroxyapatite based materials for bone tissue engineering: A brief and comprehensive introduction. *Crystals*, 11(2), 149.
30. Kang, S., Haider, A., Gupta, K. C., Kim, H., & Kang, I. (2022). Chemical bonding of biomolecules to the surface of nano-hydroxyapatite to enhance its bioactivity. *Coatings*, 12(7), 999.
31. Dutta, S. R., Passi, D., Singh, P., &Bhuibhar, A. (2015). Ceramic and non-ceramic hydroxyapatite as a bone graft material: a brief review. *Irish Journal of Medical Science (1971-)*, 184, 101-106.
32. Lett, J. A., Sagadevan, S., Fatimah, I., Hoque, M. E., Lokanathan, Y., Léonard, E., ... & Oh, W. C. (2021). Recent advances in natural polymer-based hydroxyapatite scaffolds: Properties and applications. *European Polymer Journal*, 148, 110360.



33. Sprio, S., Dapporto, M., Preti, L., Mazzoni, E., Iaquina, M. R., Martini, F., ... & Tampieri, A. (2020). Enhancement of the biological and mechanical performances of sintered hydroxyapatite by multiple ions doping. *Frontiers in Materials*, 7, 224.